

Epipolar Resampling of Space-borne Linear Array Scanner Scenes Using Parallel Projection

Michel Morgan, Kyung-Ok Kim, Soo Jeong, and Ayman Habib

Abstract

Epipolar resampling aims at generating normalized images where conjugate points are located along the same row. Such a characteristic makes normalized imagery important for many applications such as automatic image matching, aerial triangulation, DEM and ortho-photo generation, and stereo-viewing. Traditionally, the input media for the normalization process are digital images captured by frame cameras. These images could be either derived by scanning analog photographs or directly captured by digital cameras. Current digital frame cameras provide smaller format imagery compared to those of analog cameras. In this regard, linear array scanners are emerging as a viable substitute to two-dimensional digital frame cameras. However, linear array scanners have more complex imaging geometry than that of frame cameras. In general, the imaging geometry of linear array scanners produces non-straight epipolar lines. Moreover, epipolar resampling of captured scenes according to the rigorous model, which faithfully describes the imaging process, requires the knowledge of the internal and external sensor characteristics as well as a Digital Elevation Model (DEM) of the object space. Recently, parallel projection has emerged as an alternative model approximating the imaging geometry of high altitude scanners with narrow angular field of view. In contrast to the rigorous model, the parallel projection model does not require the internal or the external characteristics of the imaging system and produces straight epipolar lines. In this paper, the parallel projection equations are modified for better modeling of linear array scanners. The modified parallel projection model is then used to resample linear array scanner scenes according to epipolar geometry. Experimental results using Ikonos and SPOT data demonstrate the feasibility of the proposed methodology.

Michel Morgan is with North West Geomatics Ltd., 212, 5438 - 11St N.E., Calgary, Alberta, T2E 7E9 Canada (michel.morgan@nwgeo.com).

Kyung-Ok Kim is with the Electronics and Telecommunications Research Institute (ETRI), 161 Gajeong-Dong, Yuseong-Gu, Daejeon, 305-350, Korea (kokim@etri.re.kr).

Soo Jeong is with the Department of Civil Engineering, College of Engineering, Andong National University, 388 Songcheon-dong, Andong, Gyeongsangbuk-do, 760-749, Korea (soo@andong.ac.kr).

Ayman Habib is with the Department of Geomatics Engineering, University of Calgary, 2500 University Drive, NW, Calgary, Alberta, Canada, T2N 1N4 (habib@geomatics.ucalgary.ca).

Introduction

Resampled images according to epipolar geometry have the prime characteristic of having conjugate points along the same row. They are utilized in many photogrammetric applications such as automatic image matching, aerial triangulation, DEM and ortho-photo generation, and stereo-viewing. To cope with the increasing demand for a shorter gap between data acquisition and product delivery, many current mapping projects are moving towards digital frame and/or line cameras. Due to technical limitations, existing digital frame cameras are smaller in format than analog cameras. Therefore, linear array scanners have emerged as a good alternative, where this limitation is compensated for through continuous exposure of one to three scan lines along the focal plane. On the negative side, the widespread incorporation of linear array scanners has led to many challenges to traditional topographic mapping applications (Fritz, 1995). The geometric modeling and normalization of linear array scanner scenes are among the key challenges facing researchers within the photogrammetric community.

The normalization procedure, as well as deriving object space information from imagery, requires mathematical modeling of the incorporated sensor. Rigorous and approximate sensor models are the two main categories describing the mathematics of the involved imaging geometry. The former is based on the actual geometry of the image formation process involving the internal Interior Orientation Parameters (IOP) and the external Exterior Orientation/geo-referencing Parameters (EOP) characteristics of the implemented sensor. Since rigorous modeling is the most accurate model, it has been the focus of a large body of photogrammetric literature (Lee and Habib, 2002; Habib *et al.*, 2001; Lee *et al.*, 2000; Wang, 1999; McGlone and Mikhail, 1981). The EOP/geo-referencing parameters can be indirectly estimated using Ground Control Points (GCP) or directly obtained using GPS/INS units. The indirect estimation of the EOP requires an excessive number of ground control points (Poli, 2003). Moreover, in indirect geo-referencing, as the Angular Field of View (AFOV) becomes small, high correlations develop between exterior orientation parameters within a perspective projection since the narrow bundle of rays effectively approaches a skew parallel projection (Fraser *et al.*, 2001; Hattori *et al.*, 2000; Wang, 1999). On the other

Photogrammetric Engineering & Remote Sensing
Vol. 72, No. 11, November 2006, pp. 1255–1263.

0099-1112/06/7211-1255/\$3.00/0

© 2006 American Society for Photogrammetry
and Remote Sensing

hand, direct geo-referencing, using GPS/INS units, is negatively affected by bias values in the available IOP and/or EOP (Fraser and Hanley, 2003; Habib and Schenk, 2001). Furthermore, the direct geo-referencing parameters might be concealed by the scene provider. For example, Space Imaging does not provide the EOP for commercially available Ikonos scenes.

Regardless of the utilized method for deriving the EOP, using the rigorous sensor model for epipolar resampling of linear array scanner scenes has the following limitations (Habib *et al.*, 2005):

- In general, rigorously derived epipolar lines in scenes captured by linear array scanners are not straight. Such a phenomenon has been proven for scanners whose trajectory is modeled by second order polynomial functions in position and heading and first order polynomial functions in pitch and roll angles (Kim, 2000), as well as scanners moving with constant velocity and attitude (Habib *et al.*, 2005). Since the normalization procedure aims at projecting the epipolar lines onto straight lines along the scene rows, resampling linear array scanner scenes according epipolar geometry is not as straightforward as in the case of frame imagery.
- Using the rigorous sensor model, there is no simple transformation function that maps non-straight epipolar lines in the original scenes onto straight ones in the normalized scenes. Moreover, the resampling procedure calls for the availability of Digital Elevation Models (DEM) together with the internal and external sensor characteristics (Habib *et al.*, 2005). The object space requirement is impractical since the normalization process is mainly carried out to facilitate DEM generation (Schenk, 1999). In addition, the internal and external sensor characteristics might not be available due to lack of the necessary control and/or intentional concealment by the scene provider, which is the case for Ikonos imagery.

The above limitations of the rigorous sensor model has led to the development of approximate models such as Rational Function Model (RFM), Direct Linear Transformation (DLT), Self-calibrating Direct Linear Transformation (SDLT), and parallel projection (Fraser *et al.*, 2001; Tao and Hu, 2001; Wang, 1999; Okamoto *et al.*, 1992; Abdel-Aziz and Karara, 1971). Among these alternative models, the parallel projection is the simplest one, which could be utilized for epipolar resampling since it accurately describes the imaging geometry of scanners with narrow AFOV moving with constant velocity and attitude.

This paper starts with a brief discussion of epipolar resampling of frame and linear array scanner imagery. This introduction is followed by the rationale behind the choice of the parallel projection model and its mathematical formulas. Then, the proposed approach for epipolar resampling of linear array scanner scenes is introduced. The experimental results section outlines the performance of the new approach in resampling Ikonos and SPOT scenes according to epipolar geometry. Finally, the paper highlights the research conclusions and recommendations for future work.

Epipolar Resampling of Frame and Linear Array Scanner

Imagery: Background

Epipolar resampling aims at generating normalized images where corresponding points are located along the same row. Moreover, the x-parallax between conjugate points in the normalized imagery is linearly proportional to the depth of the corresponding object point across the air base connecting the involved perspective centers. Prior to investigating linear array scanner scenes, one has to closely analyze the normalization process for frame images. Such an analysis is essential since it provides the conceptual bases, which are common to frame cameras and linear array scanners. Figure 1 depicts the relative relationship among the original and normalized frame

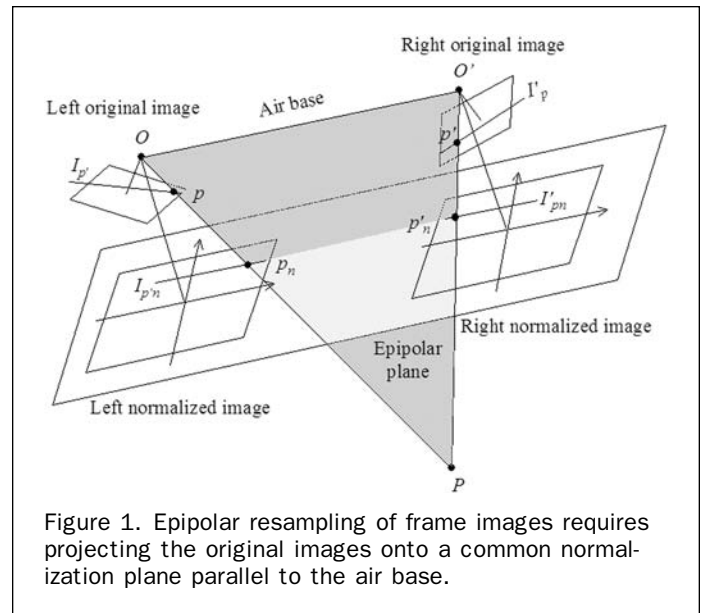


Figure 1. Epipolar resampling of frame images requires projecting the original images onto a common normalization plane parallel to the air base.

images. For a given image point (p), the epipolar plane is defined as the plane through the air base and the point in question. The intersection of the epipolar plane with the image planes produces conjugate and straight epipolar lines (I_p' , I_p). The normalization process creates new imagery where conjugate epipolar lines are aligned along the same row. According to Cho *et al.*, 1992, the resampling process can be summarized as follows, Figure 1:

- To ensure equidistance and parallel epipolar lines, a common normalization plane is selected in such a way it is parallel to the air base. The orientation of the normalization plane is established using the relative orientation parameters between the original stereo-scenes.
- The x-axis of the resampled images within the normalization plane is chosen to be parallel to the air base. Such a choice guarantees that the epipolar lines in the normalized scenes are parallel to the x-axis.
- The contents of the original images are projected onto the normalization plane. Since the previous requirements for the normalized images can be satisfied while maintaining the perspective centers of the original imagery, the transformation from the original to the normalized imagery can be realized through a projective transformation. The projective transformation parameters are completely defined by the relative orientation parameters between the original scenes.

As was mentioned in the introduction, using the rigorous sensor model for epipolar resampling of linear array scanner scenes has many limitations. Alternatively, approximate models, which do not involve the internal and external characteristics of the implemented sensor, are emerging as potential alternatives leading to a simpler normalization procedure for linear array scanner scenes. Among these models, the parallel projection seems to be the most promising as it yields straight epipolar lines (Habib *et al.*, 2005). Thus, the following sections deal with this model with regard to its suitability as an approximate sensor model and how it influences the normalization procedure.

Parallel Projection

This section starts by discussing the rationale behind the selection of the parallel projection as an approximate sensor model and its mathematics. This discussion will be followed by a necessary modification to bring the actual imaging geometry of linear array scanners closer to the parallel projection.

Rationale

The parallel projection assumes that the projection rays from the object space to the scene plane are parallel to each other. Therefore, for such an imaging geometry, there is no projection/perspective center. This would be the case if the principal distance associated with perspective projection approaches infinity; that is the sensor's AFOV approaches zero. The suitability of the parallel projection model in approximating the imaging geometry associated with linear array scanner scenes can be attributed to the following remarks (Okamoto *et al.*, 1992):

- Many space borne scanners have narrow AFOV. For example, the AFOV for an Ikonos scene is less than 1°. In such a case, the perspective light rays along the scanning direction are very close to being parallel.
- Space imagery is usually acquired within a short time period, e.g., it is about one second for an Ikonos scene. Therefore, the scanner can be assumed to have the same attitude while capturing the scene. Consequently, the perspective/planar bundles defined by consecutive scans are parallel to each other.
- For scenes captured within a very short time period, the scanner can be assumed to move with constant velocity (i.e., the scanner travels equal distances in equal time intervals).

The first observation leads to an *almost* parallel projection along the scan lines, while the remaining remarks yield parallel projection across the scan lines. In summary, one might assume that scenes captured by space-borne scanners with narrow AFOV in a short time period conform to parallel projection geometry. The mathematics of the parallel projection will be discussed in the next subsection.

Mathematical Formulation of the Parallel Projection Model

The objective of this section is to introduce the mathematical relationship between the coordinates of corresponding object and scene points in imagery captured according to parallel projection. The parallel projection model, as shown in Figure 2, involves the following eight parameters (Morgan *et al.*, 2004b):

- Two components of the unit vector along the projection direction (L, M);
- Orientation angles of the scene coordinate system (ω, φ, κ);
- Two shift values ($\Delta x, \Delta y$); and
- Scale factor (s).

The parallel projection model relating an object point, $P(X, Y, Z)$, to its scene point, $p(u, v, 0)$, can be expressed as:

$$\begin{bmatrix} u \\ v \\ 0 \end{bmatrix} = s \cdot \lambda \cdot R_{(\omega, \varphi, \kappa)}^T \begin{bmatrix} L \\ M \\ N \end{bmatrix} + s \cdot R_{(\omega, \varphi, \kappa)}^T \begin{bmatrix} X \\ Y \\ Z \end{bmatrix} + \begin{bmatrix} \Delta x \\ \Delta y \\ 0 \end{bmatrix} \quad (1)$$

where: λ is the distance between the object point P and the corresponding scene point p ; $R_{(\omega, \varphi, \kappa)}$ is the rotation matrix between the scene and object coordinate systems; and N is the Z -component of the unit projection vector, i.e., $N = \sqrt{1 - L^2 - M^2}$; λ can be eliminated by computing its value from the third equation in Equation 1 and substituting in the first and second equations. This produces the linear form of the parallel projection, Equations 2:

$$\begin{aligned} u &= A_1 X + A_2 Y + A_3 Z + A_4 \\ v &= A_5 X + A_6 Y + A_7 Z + A_8 \end{aligned} \quad (2)$$

The coefficients A_1 to A_8 in Equations 2 represent the linear parallel projection parameters corresponding to ($L, M, \omega, \varphi, \kappa, \Delta x, \Delta y, \text{ and } s$). Forward and backward transformations between these sets of parameters could be easily developed (Morgan *et al.*, 2004b). It should be noted that Equations 1

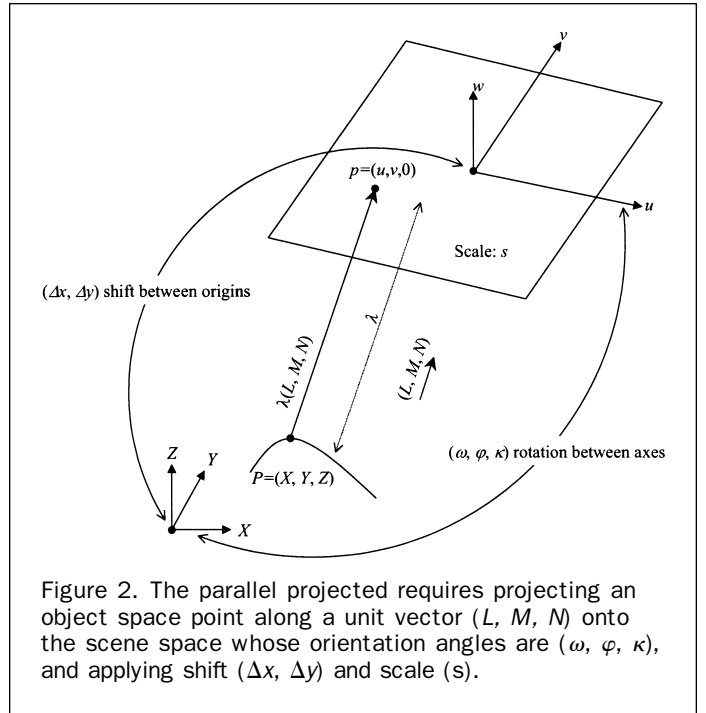


Figure 2. The parallel projected requires projecting an object space point along a unit vector (L, M, N) onto the scene space whose orientation angles are (ω, φ, κ), and applying shift ($\Delta x, \Delta y$) and scale (s).

and 2 describe the mathematical relationship between a three-dimensional object space and a two-dimensional scene. An extension of this model deals with a planar object space. In this case, the Z component of the object coordinates can be expressed as a linear combination of the planimetric coordinates (X and Y). Thus, the parallel projection between two planes is represented by a 6-parameter Affine transformation as expressed in Equations 3:

$$\begin{aligned} u &= A_1' X + A_2' Y + A_3' \\ v &= A_4' X + A_5' Y + A_6' \end{aligned} \quad (3)$$

Perspective to Parallel (PTP) Transformation

The imaging geometry of scenes captured by a scanner moving along its trajectory with constant velocity and attitude can be described by a parallel projection along the flight trajectory and perspective geometry along the scanner direction. The perspective projection along the scanner direction can be approximated by a parallel projection for systems with narrow AFOV. However, the scene coordinates along the scan line direction can be modified to bring the perspective projection along the scan line closer to being a parallel one. This modification can be established through Perspective to Parallel (PTP) transformation (Okamoto *et al.*, 1992), as expressed by the first equation in Equations 4. The second equation in Equations 4 indicates that no modification is required across the scan lines since the system is assumed to travel with constant velocity and attitude.

$$\begin{aligned} v &= y \frac{1}{1 - \frac{y}{c} \tan(\psi)} \\ u &= x \end{aligned} \quad (4)$$

where c is the scanner's principal distance; ψ is the scanner roll angle; and x, y are the original scene coordinates across and along the scan line, respectively.

It should be noted that the PTP in Equations 4 assumes a *flat terrain* (Okamoto *et al.*, 1992). For non-flat terrain, Equations 4 will result in transformation errors in the scene

coordinates. Okamoto *et al.* (1992) derived a quantitative measure of these errors as function of the height variation of the object space. It was found that a transformation error of less than 5 μm can be achieved for SPOT scenes if terrain variation does not exceed 300 m. For Ikonos scenes, same level of accuracy can be achieved if height variation does not exceed 50 m. Combining the linear form of the parallel projection and the PTP transformation yields the modified parallel projection in Equations 5:

$$\begin{aligned}
 x &= A_1X + A_2Y + A_3Z + A_4 \\
 y &= \frac{A_5X + A_6Y + A_7Z + A_8}{1 + \frac{\tan(\psi)}{c}(A_5X + A_6Y + A_7Z + A_8)}. \quad (5)
 \end{aligned}$$

The nine parameters in Equations 5 (A_1 to A_8 and ψ) can be estimated using a minimum of five GCP. One should note that if the roll angle (ψ) is available from the navigation data, it could be used directly in Equations 4 or 5. The next section deals with the utilization of the parallel projection parameters for epipolar resampling of linear array scanner scenes.

Parallel Projection for Epipolar Resampling of Linear Array Scanner Scenes

Normalization Plane Selection

Before discussing the epipolar resampling approach, one has to reintroduce the concept of epipolar plane to suit the parallel projection model. For stereo-scenes generated according to parallel projection, the epipolar plane for a given object/scene point can be defined by that point and the projection vectors for the left and right scenes. Figure 3 shows epipolar planes for two object space points. From the figure, one can see that the intersection of the epipolar planes with the scene planes yields straight epipolar lines. In addition, since the projection vectors are constant for

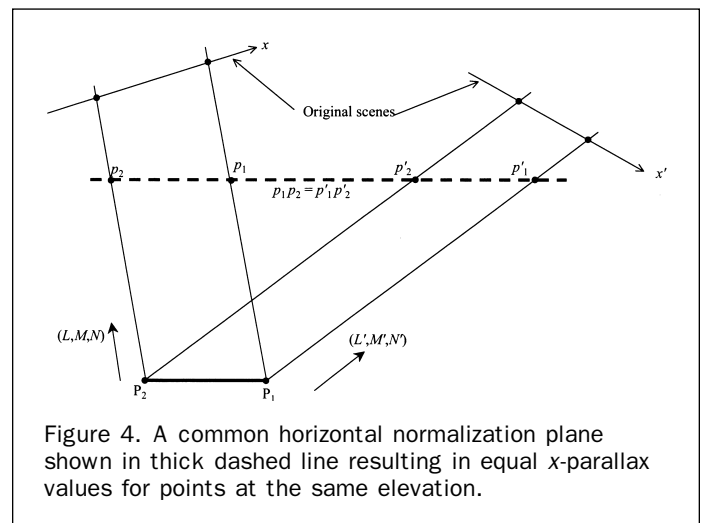
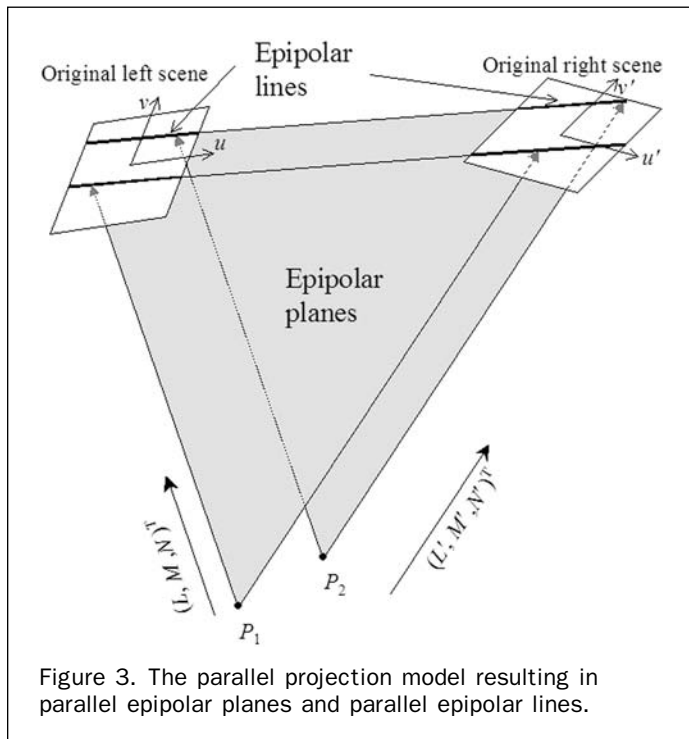
a given stereo-pair, Figure 3 shows that epipolar planes associated with different points are parallel to each other. Thus, epipolar lines within the same scene are parallel to each other. Morgan *et al.*, 2004a, derived a methodology for rotating, scaling, and shifting the scenes in order to eliminate y -parallax between the scenes. However, this methodology is incapable of providing a linear relationship between x -parallax and depth values.

Recall that in the case of frame cameras, a common normalization plane was chosen on which the images are projected during the normalization procedure. Similarly, in the case of linear array scanners, we would like to choose a plane to project the scenes. The selection criterion is to maintain a linear relationship between x -parallax and depth values. Figure 4 depicts a profile along the epipolar plane containing two object points P_1 and P_2 at the same elevation. The figure also shows the epipolar line pairs for non-coplanar and coplanar stereo-scenes. A closer investigation of this figure reveals that the same x -parallax value for these points could be only achieved when dealing with stereo-scenes contained within a common horizontal plane (as represented by the bold dashed line in Figure 4). Therefore, scenes contained in a *common* and *horizontal* plane will exhibit x -parallax values that are linearly proportional to the *elevation*. This common plane will be denoted hereafter as the normalization plane.

The question now is how to project the original scenes onto the normalization plane. Since the parallel projection between two planes is modeled by a 6-parameter Affine transformation, the projection of the original scene onto the normalization plane can be realized through the transformation in Equations 3. In addition, the projected scenes should be rotated, scaled, and shifted within the normalization plane to guarantee that conjugate epipolar lines are along same rows. It should be noted that a transformation involving planar rotation, scaling, and shifting is a subset of Affine transformation. Due to the transitive property of the Affine transformation, the projection onto the normalization plane and the in-plane rotation, scale, and shift can be combined into one 6-parameter Affine transformation. Therefore, the normalization procedure hinges on the determination of the Affine transformation parameters between the original and normalized scenes. The determination of these parameters will be the focus of the next subsection.

Normalization Procedure

So far, we have established the following facts for captured scenes according to parallel projection:

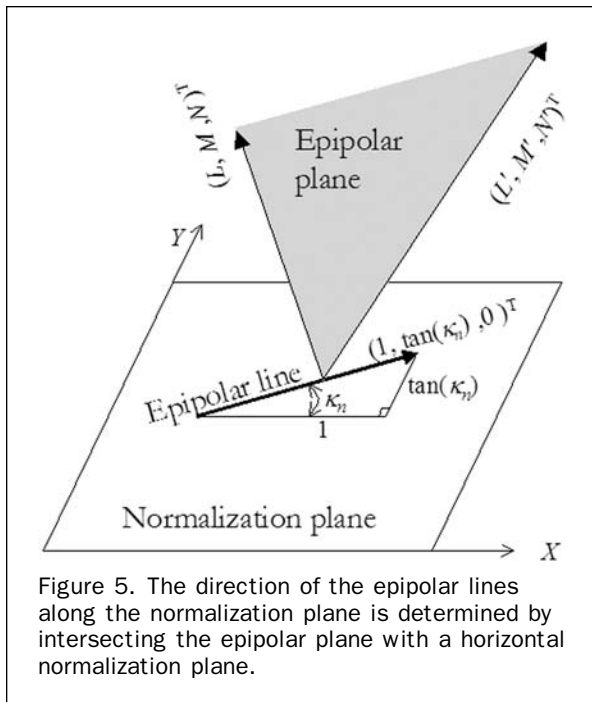


- The epipolar lines are straight.
- Within the same scene, the epipolar lines are parallel to each other.
- To ensure a meaningful relationship between the x-parallax and depth information, the original scenes should be projected onto a common horizontal plane (normalization plane).
- The y-parallax between conjugate points/epipolar lines can be eliminated by in-plane transformation involving rotation, scale, and shift.
- The transformation from the original scenes to the normalized ones can be established in a one single step, by combining the parameters from the last two transformations.

The question to be addressed in this section is how to estimate the affine transformation parameters, which directly project the original scenes onto the normalized ones. First, the left and right scene planes should be contained within a common horizontal plane. Thus, the orientation angles (ω_n, φ_n) of the normalization plane should be zero. Second, the x-axis of the scene coordinate system should be parallel to the direction of the epipolar lines. This is essential for having the epipolar lines aligned along the scene rows. The direction of the x-axis within the scene is defined by the rotation angle (κ_n). So, the (κ_n) value should be determined in such a way that the x-axis coincides with the epipolar lines. The direction of the epipolar lines can be determined by intersecting the epipolar plane (the plane containing the projection vectors (L, M, N) and (L', M', N')) with the normalization plane. Figure 5 shows that the intersection of the epipolar plane and a horizontal normalization plane determines the orientation of the epipolar lines ($1, \tan(\kappa_n), 0$). Equation 6 indicates that the projection vectors and the epipolar lines are coplanar:

$$\begin{vmatrix} L & M & N \\ L' & M' & N' \\ 1 & \tan(\kappa_n) & 0 \end{vmatrix} = 0. \quad (6)$$

Thus, the numerical value for (κ_n) can be determined according to Equation 7:



$$\kappa_n = \arctan\left(\frac{N.M' - M.N'}{N.L' - L.N'}\right). \quad (7)$$

To ensure that conjugate epipolar lines are aligned along the same rows, the left and right scenes should have the same scale (s_n) and the same shift along the y-axis (Δy_n). The shift value along the x-axis is irrelevant but it could be chosen to be the same for both scenes (Δx_n). In summary, selecting ($L, M, \omega_n, \varphi_n, \kappa_n, \Delta x_n, \Delta y_n, s_n$) and ($L', M', \omega_n, \varphi_n, \kappa_n, \Delta x_n, \Delta y_n, s_n$) as the parallel projection parameters from the object space to the left and right scenes, respectively, would ensure the generation of normalized scenes.

Having introduced the necessary conditions for a direct generation of normalized scenes through parallel projection, we would like to establish the relationship between corresponding points in the original and normalized scenes. This relationship could be derived by considering the respective parallel projection parameters as well as the mathematical model for the parallel projection (Equations 1). Equations 8 introduce such a relationship when considering the left original and normalized scenes:

$$\begin{aligned} \begin{bmatrix} X \\ Y \\ Z \end{bmatrix} &= \frac{1}{s} R_{(\omega, \varphi, \kappa)} \begin{bmatrix} u - \Delta x \\ v - \Delta y \\ 0 \end{bmatrix} - \lambda \begin{bmatrix} L \\ M \\ N \end{bmatrix} \\ &= \frac{1}{s_n} R_{(\omega_n, \varphi_n, \kappa_n)} \begin{bmatrix} u_n - \Delta x_n \\ v_n - \Delta y_n \\ 0 \end{bmatrix} - \lambda_n \begin{bmatrix} L \\ M \\ N \end{bmatrix}. \end{aligned} \quad (8)$$

Equations 8 can be reduced to the form in Equations 9 through the elimination of the object coordinates (X, Y, Z):

$$\begin{aligned} \begin{bmatrix} u_n \\ v_n \\ 0 \end{bmatrix} &= \begin{bmatrix} \Delta x_n \\ \Delta y_n \\ 0 \end{bmatrix} + s_n(\lambda_n - \lambda) R_{(\omega_n, \varphi_n, \kappa_n)}^T \begin{bmatrix} L \\ M \\ N \end{bmatrix} \\ &+ \frac{s_n}{s} R_{(\omega_n, \varphi_n, \kappa_n)}^T R_{(\omega, \varphi, \kappa)} \begin{bmatrix} u - \Delta x \\ v - \Delta y \\ 0 \end{bmatrix}. \end{aligned} \quad (9)$$

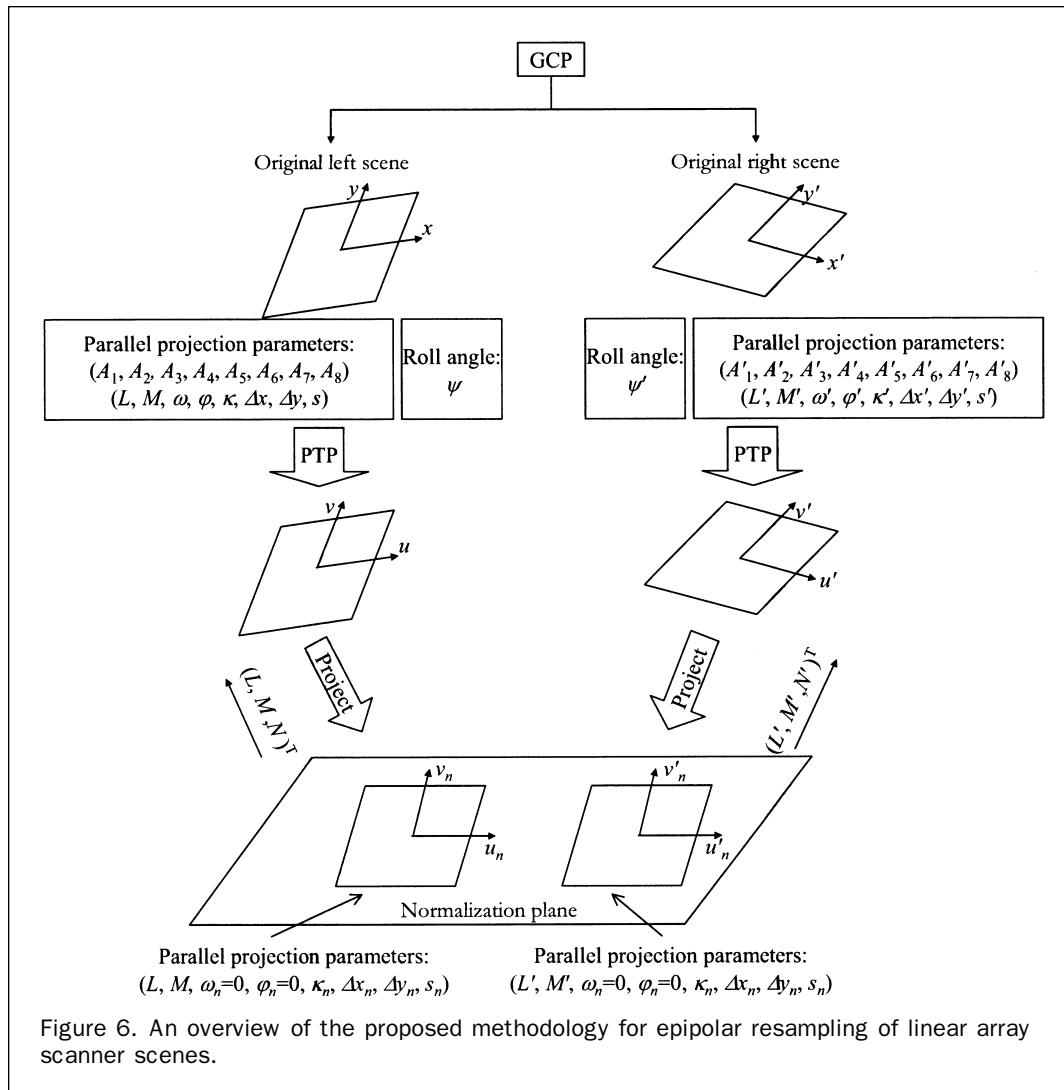
Equations 9 represent the relationship between the original and normalized scene coordinates (u, v, u_n, v_n) as a function of the parallel projection parameters of the original and normalized scenes. The term ($\lambda_n - \lambda$) can be computed from the third equation in Equations 9 and reintroduced in the first two equations resulting in a 6-parameter affine transformation between original and normalized scene coordinates, Equations 10:

$$\begin{aligned} u_n &= a_1 u + a_2 v + a_3 \\ v_n &= a_4 u + a_5 v + a_6. \end{aligned} \quad (10)$$

In Equations 10, the parameters (a_1 to a_6) are directly derived from the parallel projection parameters for the original and normalized scenes ($L, M, \omega, \varphi, \kappa, \Delta x, \Delta y, s$) and ($L, M, \omega_n, \varphi_n, \kappa_n, \Delta x_n, \Delta y_n, s_n$), respectively. A similar transformation can be derived for the right scene.

In summary, the normalization process could proceed as follows (refer to Figure 6 for a conceptual flow chart):

1. Use a minimum of five ground control points to estimate the nine parameters of the modified parallel projection (A_1 to A_8 and ψ in Equations 5) for the left and right scenes in question.



2. Use the estimated roll angles in step 1 to perform the PTP transformation for the left and right scenes, Equations 4.
3. Use the estimated parameters in step 1 to derive the corresponding non-linear parameters of the parallel projection for the left and right scenes ($L, M, \omega, \varphi, \kappa, \Delta x, \Delta y, s$) and ($L', M', \omega', \varphi', \kappa', \Delta x', \Delta y', s'$), respectively.
4. Select the parallel projection parameters for the left and right normalized scenes ($L, M, \omega_n, \varphi_n, \kappa_n, \Delta x_n, \Delta y_n, s_n$) and ($L', M', \omega_n, \varphi_n, \kappa_n, \Delta x_n, \Delta y_n, s_n$), respectively. To ensure an x-parallax that is linearly proportional to the elevation, we should select a horizontal normalization plane (i.e., $\omega_n = \varphi_n = 0$). The (κ_n) value should be derived according to Equation 7. The shift and scale values ($\Delta x_n, \Delta y_n, s_n$) can be selected to be the average scale and shift values for the original left and right scenes.
5. Use the original and the normalized parallel projection parameters to derive the affine transformation parameters (Equations 10), which are used for directly projecting the original scenes after PTP transformation onto the normalized ones.

It should be noted that the requirement for the GCP is to ensure the alignment of the normalized scenes along a common plane. This alignment leads to x-parallax values that are linearly proportional to the depth across the normalization plane. In addition, GCP are needed to estimate the roll angles. Such angles are used to perform the PTP transformation, which is a pre-requisite for utilizing the parallel projection.

Experimental Results and Discussion

The main objectives of the conducted experiments revolve around proving the feasibility of the suggested approach and evaluating the accuracy of the resampling process as it is impacted by the number of utilized GCP. To achieve such objectives, two sets of experiments were performed on Ikonos and SPOT data.

Experimental Results for Ikonos Data

We acquired a panchromatic stereo-pair of Ikonos scenes over Daejeon, South Korea. The geographical coordinates of the covered area range from 36.26° to 36.36° North Latitude and from 127.31° to 127.45° East Longitude. Some of the scenes' specifications are listed in Table 1. For these

TABLE 1. SPECIFICATIONS OF IKONOS AND SPOT DATASETS USED IN THE EXPERIMENTS

Dataset	I		II	
	Ikonos Left	Ikonos Right	SPOT-1 Left	SPOT-2 Right
Number of rows	13824	14336	6000	6000
Number of columns	13816	13816	6000	6000
Pixel size, μm	10	10	13	13
Ground resolution, m	1	1	10	10

TABLE 2. EXPERIMENTAL RESULTS OF THE NORMALIZATION PROCESS OF IKONOS AND SPOT SCENES

Experiment #	Ikonos			SPOT		
	1	2	3	4	5	6
# of GCP	9	25	162	6	16	26
# of Checkpoints	153	137	0	20	10	0
$\hat{\sigma}_0$, pixels	3.6	2.8	2.2	<0.5	<0.5	<0.5
Mean $ P_y $, pixels	2.1	1.7	1.5	0.8	0.5	0.4
Max $ P_y $, pixels	11.6	9.8	8.3	4.8	2.2	1.2
$\hat{\sigma}_0$ (line fitting of P_x and Z), m	6.0	5.6	5.4	3.8	2.7	2.6

scenes, we do not have any information regarding the roll angles or any GCP. Instead, the rational function coefficients for both scenes are provided. The rational function coefficients are used in an intersection procedure to derive the ground coordinates of 162 well-distributed manually digitized points. In the following experiments, some of these coordinates will be used as GCP and the rest will be used as checkpoints. It should be noted that the accuracy of the estimated ground coordinates for these points depends on:

- The measurement accuracy of the scene coordinates;
- The accuracy of the rational functions' coefficients (not provided); and
- The validity of the rational functions as an approximate sensor model.

Before implementing the proposed epipolar resampling methodology, we tested the original scenes, and we found that average y -parallax values is 175 pixels. The developed approach for epipolar resampling is then applied to generate normalized stereo-scenes. Three sets of results using different numbers of GCP and checkpoints are shown in Table 2. The square root of the estimated variance component resulting from the least squares adjustment adopting Equations 5, and the average absolute values of the resulting y -parallax in the resampled scenes for the 162 points are listed in Table 2. Recall that one of the objectives is to achieve linear relationship between x -parallax and depth values. Thus, the table also shows the square root of the estimated variance component from straight-line fitting through the pairs defined by the resulting x -parallax in the normalized scenes and the corresponding depth values. One has to note that these numerical values reflect the quality of the used GCP, the accuracy of scenes coordinate measurements, and the validity of the modified parallel projection model (including the assumption of a flat terrain). Close investigation of these numbers reveals that increasing the number of GCP improves the results as indicated by smaller variance component and absolute y -parallax values. However, one can argue that there is an insignificant improvement between Experiment 2 (using 25 GCP) and Experiment 3 (using 162 GCP). Thus, it can be concluded that few GCP are sufficient to carry out the proposed epipolar resampling methodology. The quality of the line fitting between the x -parallax and corresponding depth, as represented by the last row in Table 2, is acceptable considering the inaccuracies introduced by various errors throughout the normalization process (e.g., errors in the object and scene coordinates as well as those arising from the deviation from a planar object space assumption in the PTP transformation). Finally, the resampled scenes are overlaid to

generate a stereo anaglyph, Figure 7, which can be stereoviewed using anaglyph glasses.

Experimental Results using SPOT Data

The second dataset involves a stereo-pair captured by SPOT-1 and SPOT-2 over Korea. The specifications of these scenes are listed in Table 1. Twenty-six well-distributed GCP have been collected through a triangulation procedure involving aerial imagery over the same area. It is important to mention that these GCP are of higher accuracy/reliability than those obtained for Ikonos data. For the original scenes, average y -parallax values of these points was 267 pixels. The epipolar resampling approach was implemented and three sets of results were obtained, Table 2, by changing the number of GCP. Similar to Ikonos results, as the number of GCP increases, the accuracy increases, in terms of smaller y -parallax and better linear relationship between x -parallax and height values. One can also notice insignificant improvement of these values due to increasing the number of GCP from 16 (in Experiment 5) to 26 (in Experiment 6). For all SPOT experiments, we could achieve high accuracy in the image and object space (attributed to the highly accurate and reliable GCP), which confirms the validity of the modified parallel projection model and the developed epipolar resampling approach.

Conclusions and Recommendations for Future Research

This paper outlines a new approach for epipolar resampling of space-borne linear array scanners scenes. The resampling process is based on parallel projection, which is suitable for modeling imaging scanners with narrow AFOV moving with constant velocity and attitude. The original scenes should undergo a Perspective to Parallel (PTP) transformation to bring the perspective geometry along the scanner direction closer to being parallel. The parallel projection and PTP transformation have been combined into a modified parallel projection model. The involved parameters in the combined model can be estimated using a minimum of five GCP.

It has been established that the epipolar lines in scenes captured according to parallel projection are straight lines and parallel to each other. The generation of normalized scenes, where there is no y -parallax between conjugate points and a meaningful x -parallax value that is linearly proportional to the depth requires projecting the original scenes onto a common plane followed by an in-plane transformation. The transformation from the original scenes into normalized ones can be directly established through a 6-parameter affine transformation using a minimum of five GCP. Experimental results with Ikonos and SPOT imagery verified the feasibility and success of the proposed resampling procedure.

Future work will focus on DEM and orthophoto generation based on the normalized scenes. Inclusion of higher order primitives (such as linear and areal features) and object space constraints within the parallel projection model will also be investigated. Moreover, we will investigate the effect of the deviations from the assumptions in the PTP transformation (especially, the flat terrain). In addition, we will look into the possibility of eliminating the need for GCP to carry out the normalization procedure through relative orientation of stereo-scenes captured according to parallel projection.

References

- Abdel-Aziz, Y., and H. Karara, 1971. Direct linear transformation from comparator coordinates into object space coordinates in close-range photogrammetry, *Proceedings of ASP/UI Sympo-*

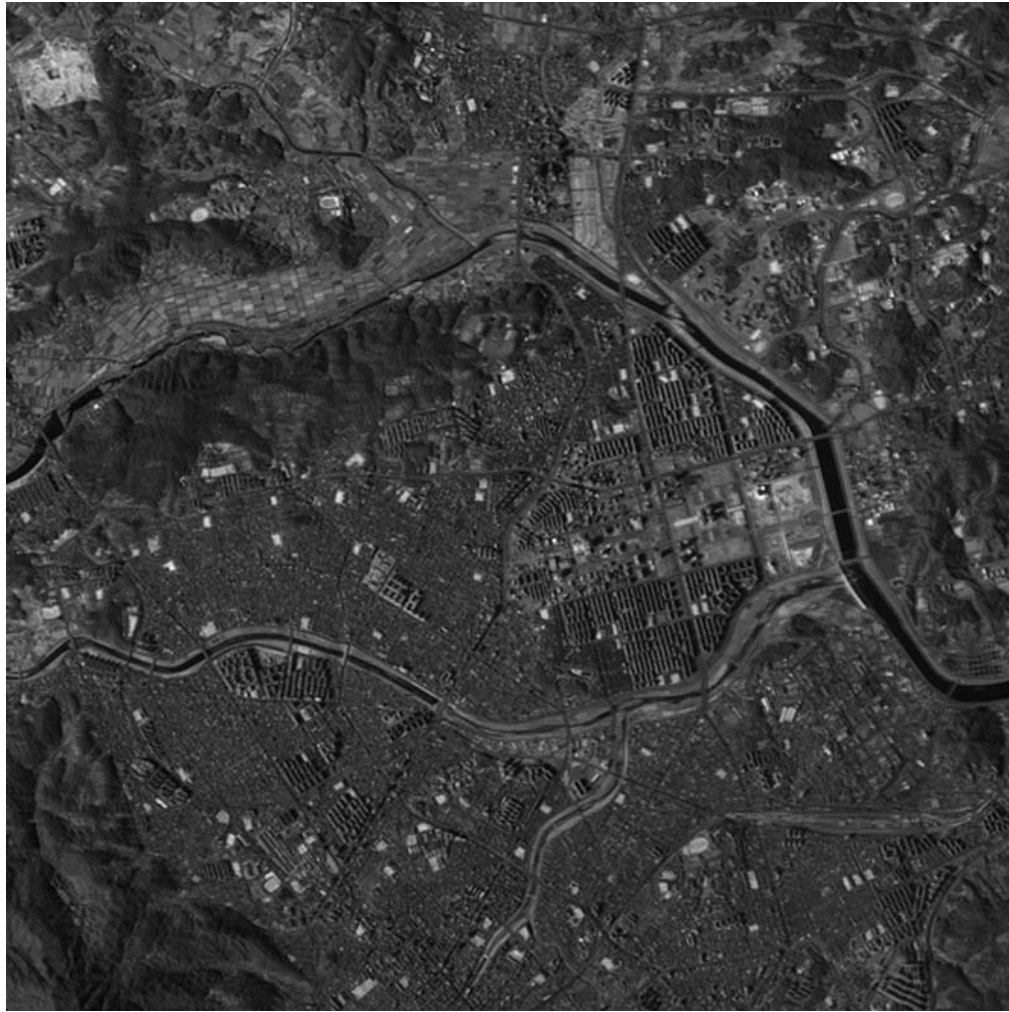


Figure 7. Generated stereo anaglyph from the normalized Ikonos scenes. A color version of this figure is available at the ASPRS website: www.asprs.org.

- sium on Close Range Photogrammetry*, 26–29 January, University of Illinois at Urbana Champaign, Urbana, Illinois, pp. 1–18.
- Cho, W., T. Schenk, and M. Madani, 1992. Resampling digital imagery to epipolar geometry, *IAPRS International Archives of Photogrammetry and Remote Sensing*, 02–14 August, Washington, D.C., 29(B3):404–408.
- Fraser, C., H. Hanley, and T. Yamakawa, 2001. Sub-metre geopositioning with IKONOS GEO imagery, *ISPRS Joint Workshop on High Resolution Mapping from Space*, 19–21 September, Hanover, Germany, unpaginated CD-ROM.
- Fraser, C., and H. Hanley, 2003. Bias compensation in rational functions for Ikonos satellite imagery, *Photogrammetric Engineering & Remote Sensing*, 69(1):53–57.
- Fritz, L., 1995. Recent developments for optical Earth observation in the United States, *Photogrammetric Week*, 11–15 September, Stuttgart, Germany, pp. 75–84.
- Habib, A., Y. Lee, and M. Morgan, 2001. Bundle adjustment with self-calibration of line cameras using straight lines, *Joint Workshop of ISPRS WG I/2, I/5 and IV/7: High Resolution Mapping from Space 2001*, 19–21 September, University of Hanover, Hanover, Germany, unpaginated CD-ROM.
- Habib, A., M. Morgan, S. Jeong, and K. Kim, 2005. Analysis of epipolar geometry in linear array scanner scenes, *The Photogrammetric Record*, 20(109):27–47.
- Habib, A., and T. Schenk, 2001. Accuracy analysis of reconstructed points in object space from direct and indirect exterior orientation methods, *OEEPE Workshop on Integrated Sensor Orientation*, Institute for Photogrammetry and Engineering Surveying, 17–18 September, University of Hanover, unpaginated CD-ROM.
- Hattori, S., T. Ono, C. Fraser, and H. Hasegawa, 2000. Orientation of the high resolution satellite images based on affine transformation, *Proceedings of the XIXth ISPRS Congress*, 16–23 July, Amsterdam, The Netherlands, 33(B3):359–366.
- Kim, T., 2000. A study on the epipolarity of linear pushbroom images, *Photogrammetric Engineering & Remote Sensing*, 66(8):961–966.
- Lee, Y., and A. Habib, 2002. Pose estimation of line cameras using linear features, *ISPRS Symposium of PCV '02 Photogrammetric Computer Vision*, 09–13 September, Graz, Austria, unpaginated CD-ROM.
- Lee, C., H. Theiss, J. Bethel, and E. Mikhail, 2000. Rigorous mathematical modeling of airborne pushbroom imaging systems, *Photogrammetric Engineering & Remote Sensing*, 66(4): 385–392.
- McGlone, C., and E. Mikhail, 1981. *Photogrammetric Analysis of Aircraft Multispectral Scanner Data*, School of Civil Engineering, Purdue University, West Lafayette, Indiana, 178 p.
- Morgan, M., K. Kim, S. Jeong, and A. Habib, 2004a. Indirect epipolar resampling of scenes using parallel projection modeling of

- linear array scanners, *Proceedings of the XXth ISPRS Congress*, 12–23 July, Istanbul, Turkey, 35(B3):58–513.
- Morgan, M., K. Kim, S. Jeong, and A. Habib, 2004b. Parallel projection modelling for linear array scanner scenes, *Proceedings of the XXth ISPRS Congress*, 12–23 July, Istanbul, Turkey, 35(B3):52–57.
- Okamoto, A., S. Akamatsu, H. Hasegawa, 1992. Orientation theory for satellite CCD line-scanner imagery of hilly terrains, *International Archives of Photogrammetry and Remote Sensing*, 02–14 August, Washington, D.C., Volume 29, Commission II, pp. 217–222.
- Poli, D., 2003. Georeferencing of CCD linear array sensors imagery, *Proceedings of the 2003 ASPRS Annual Meeting*, 05–09 May, Anchorage, Alaska, unpaginated CD-ROM.
- Schenk, T., 1999. *Digital Photogrammetry – Volume I*, Terra Science, Laurelville, Ohio, 428 p.
- Tao, V., and Y. Hu, 2001. A comprehensive study for rational function model for photogrammetric processing, *Photogrammetric Engineering & Remote Sensing*, 67(12):1347–1357.
- Wang, Y., 1999. Automated triangulation of linear scanner imagery, *Joint Workshop of ISPRS WG I/1, I/3 and IV/4 on Sensors and Mapping from Space*, 27–30 September, Hanover, Germany, unpaginated CD-ROM.

(Received 09 May 2005; accepted 21 July 2005; revised 02 September 2005)